A Theoretical Investigation of the Structure and Bonding of Diazomethane, CH_2N_2

Aristotle Papakondylis and Aristides Mavridis*

Laboratory of Physical Chemistry, Department of Chemistry, National and Kapodistrian University of Athens, P.O. Box 64 004, 157 10 Zografou, Athens, Greece

Received: August 18, 1998; In Final Form: October 16, 1998

We have investigated the electronic ground-state structure and binding mode of CH_2N_2 by ab initio multireference perturbation calculations CASPT2 and CASPT3, using correlation consistent cc-pVTZ basis sets. Our calculations suggest that the CH_2-N_2 binding between the CH_2 ($\tilde{a}^1A_1$) and N_2 ($X^1\Sigma_g^+$) moieties consists of a "harpooning" σ, bond from N_2 to CH_2 and a π-like bond due to the back-transfer of electrons from CH_2 to N_2. Despite the popular dipolar resonance structures employed to represent the CH_2N_2 binding no charge transfer between the in situ CH_2 and N_2 is observed. Our CH_2-N_2 dissociation energy is $D_e = 38.2$ kcal/mol with respect to the CH_2 ($\tilde{a}^1A_1$) + N_2 ($X^1\Sigma_g^+$) adiabatic products or $D_e = 27.2$ kcal/mol with respect to the ground $\tilde{X}^3B_1$ state of CH_2. Taking into account zero point energy corrections, this value is reduced to $D_o = 21.6$ kcal/mol.

Introduction

Diazomethane (CH_2N_2) was first isolated in 1894.[1] It provided organic chemists with a very versatile synthetic reagent, particularly in the methylation of acids, alcohols, and phenols. Diazomethane is a yellow gas boiling at about 0 °C[2], highly toxic and explosive under certain conditions[3]. Its electronic structure is usually described as a closed shell "resonance hybrid"[4] of the forms:

$$^{-}{:}CH_2-\overset{+}{N}\equiv N: \leftrightarrow CH_2=\overset{+}{N}=N:^{-}$$

admittedly not a very illuminating description. Considering that the molecule is composed of N_2, one of the most robust diatomics ($X^1\Sigma_g^+$, $D_e = 9.76$ eV[5]), and the CH_2 biradical, its binding mode defies a conventional description. Although quite a few theoretical papers have appeared with the purpose of elucidating the electronic structure of the ground state of CH_2N_2,[6−20] there does not seem to exist a convergence of opinion upon the matter. In addition, concerning the CH_2-N_2 bond dissociation energy, the existing experimental and/or theoretical data are in conflict.[21−27]

Most of the theoretical papers published employ small basis sets (minimal to DZ) in conjunction with the Hartree−Fock (HF) methodology and very limited CIs. Walsh and Goddard,[9] using a GVB(PP)-CI approach with a DZ basis and the experimental equilibrium geometry,[28] suggest that the CH_2N_2 ground state is a singlet biradical ($H_2\dot{C}-\dot{N}=\dot{N}:$), with the in situ CH_2 moiety in the ground $^3B_1$ state and the N_2 in its $B^3\Pi_g$ state. Notice that the experimental energy separation of N_2 ($B^3\Pi_g \leftarrow X^1\Sigma_g^+$) is 7.39 eV,[5] rendering the biradical hypothesis strongly questionable. Gerratt and co-workers,[14,15,20] using a DZ+P basis (at the experimental geometry) and their spin-coupled methodology, strongly oppose Goddard's biradical conjecture. They rather suggest that the bonding between the CH_2 and N_2 entities is caused by an in situ "hypervalent" state of the central nitrogen atom coupled to the methylene radical and to the ^4S state of the terminal nitrogen.

Bigot et al.[11,12] constructed potential energy surfaces (PES) of the reaction $CH_2 + N_2 \rightarrow CH_2N_2$ at the HF/STO-3G minimal basis level and very limited CI, but do not seem to suggest any bonding mechanism. Also, Lievin and Verhaegen[10] investigated the PESs of the same reaction using extensively a minimal STO-3G basis and a DZ basis for selective points of the surface at the HF level of theory. More recently, v. R. Schleyer et al.[16] investigated the electronic structure of CH_2N_2, mainly at the MP4/6-31G*//MP2/6-31G* level with the purpose of obtaining geometries and binding energies. On the same line of thought, Kawauchi et al.[18] performed ab initio calculations of all isomers of the CH_2N_2 system at the MP4/6-31G**//MP2/6-31G** level.

The above discussion shows clearly the need for a more thorough investigation of the diazomethane molecular system. Focusing on the binding mechanism of $CH_2 + N_2$ and taking into account the relevant low-lying states of CH_2, we have performed high level ab initio calculations; in addition, an effort was made to determine a more accurate value of the CH_2-N_2 binding energy.

Methodology

For all atoms the correlation consistent cc-pVTZ basis sets of Dunning and co-workers were used:[29,30] $((5s2p1d)_H/(10s5p2d1f)_{C,N})$, generalized contracted to $[(3s2p1d)_H/(4s3p2d1f)_{C,N}]$, i.e., 118 spherical Gaussian functions (five d and seven f functions).

Deeming as mandatory a multireference description of the molecule, the CASPT2 and CASPT3 (complete active space perturbation theory) methodology was followed.[31] At the C_s symmetry the HF configuration of diazomethane is given by the allocation

$$\tilde{X}^1A' = (\text{core})^6\,(4a')^2(5a')^2(6a')^2(7a')^2(8a')^2(9a')^2(1a'')^2\,(2a'')^2$$

The valence space of CH_2N_2 contains $16e^-$, 4 of which are involved in the two C−H bonds. A 12 e^--to-12 orbital CAS is composed of ∼114 000 configuration functions (CF), rendering a subsequent "dynamical" correlation treatment intractable. Judging the remaining 2 valence electrons of the C atom and the σ pair (∼2s) of the N_2 moiety as the most important for the CH_2-N_2 bond description, a 4 e^--to-4 orbital CAS was selected giving rise to 20 CFs. Such an approach is capable of describing adequately the interaction between the CH_2 and N_2 fragments, while at infinity a correct SCF description of the $X^1\Sigma_g^+$ state of N_2 plus a two configuration $\tilde{a}^1A_1$ state of CH_2 is obtained.

10.1021/jp983403i CCC: $18.00
Published on Web 12/19/1998

TABLE 1: Energies E (hartrees), Bond Distances r_e (angstroms) and Angles θ_e (degrees), and Energy Gaps T_e (kcal/mol) of the $\tilde{X}^3B_1$, $\tilde{a}^1A_1$, $\tilde{b}^1B_1$, and $\tilde{c}^1A_1$ States of CH_2

method	$-E$	r_e	θ_e	T_e
		$\tilde{X}^3B_1$		
CASPT2	39.06324	1.0755	133.15	0.0
CASPT3	39.07365	1.0760	133.41	0.0
TZ2P-Full CI[a]	39.06674	1.0775	133.29	0.0
experiment[b]		1.0753	133.93	0.0
		$\tilde{a}^1A_1$		
CASPT2	39.04028	1.1045	101.98	14.41
CASPT3	39.05606	1.1064	101.94	11.04
TZ2P-Full CI[a]	39.04898	1.1089	101.89	11.14
experiment		1.107[c]	102.4[c]	9.22[d]
		$\tilde{b}^1B_1$		
CASPT2	39.00773	1.072	143.8	34.83
CASPT3	39.01993	1.073	142.5	33.71
TZ2P-Full CI[a]	39.01006	1.075	141.6	35.57
experiment		1.086	139.3[e]	32.55[f]
		$\tilde{c}^1A_1$		
CASPT2	38.96618	1.0660	163.20	60.91
CASPT3	38.97661	1.0653	172.05	60.89
TZ2P-Full CI[a]	38.96847	1.0678	170.08	61.66
experiment				

[a] Reference 33b. [b] Predictions using the MORBID Hamiltonian fit to experimental data, ref 34. [c] Reference 35. [d] Reference 34. [e] Renner model fit to experiment, zero point geometry (r_0,θ_0), ref 36. [f] Renner/SO model fit to experiment, refs 34 and 37.

Dynamical correlation out of this space was extracted through the (internally contracted) PT2 and PT3 methods.[31] The internal contraction reduces, for instance, a ~5 000 000 CFs PT space to a ~330 000 one with insignificant energy losses.

To obtain a more accurate D_e value of the process $CH_2N_2 \rightarrow CH_2$ ($\tilde{a}^1A_1$)+ N_2 ($X^1\Sigma_g^+$) a 12 e^--to-12 orbital CASSCF was performed producing about 58 000 CFs at C_{2v} symmetry. To make the PT2 and PT3 calculations out of this space feasible, a limited number of CFs was selected based on the criterion $\sum_I |C_I|^2 = 0.999$, where $\{C_I\}$ are the variational coefficients of the CASSCF expansion. The energy difference between the complete (58 000 CFs) and the limited CASSCF expansions is less than 3 mhartrees. The limited CASSCF space ranges from about 1000 CFs around equilibrium to about 70 CFs at infinity. All calculations were done with the MOLPRO suite of codes.[32]

Results and Discussion

Table 1 presents results on the four low-lying states of the methylene radical, i.e., $\tilde{X}^3B_1$, $\tilde{a}^1A_1$, $\tilde{b}^1B_1$, and $\tilde{c}^1A_1$. For reasons of comparison, results are also shown of the most recent benchmark high level calculations of Schaefer and co-workers,[33] as well as experimental numbers. Our structural results of all four states at the CASPT3 level are in respectable agreement with the Full CI/TZ2P results of Schaefer et al.[33] and with available experimental data.

Now it is helpful to represent the CH_2 states with valence bond−Lewis (vbL) icons:

$|\tilde{X}^3B_1\rangle =$ 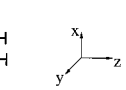 (I)

$|\tilde{a}^1A_1\rangle = c_1$ 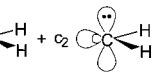 $+ c_2$ (II)

$|\tilde{b}^1B_1\rangle =$ (III)

$|\tilde{c}^1A_1\rangle = c_1'$ 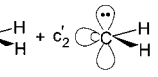 $+ c_2'$ (IV)

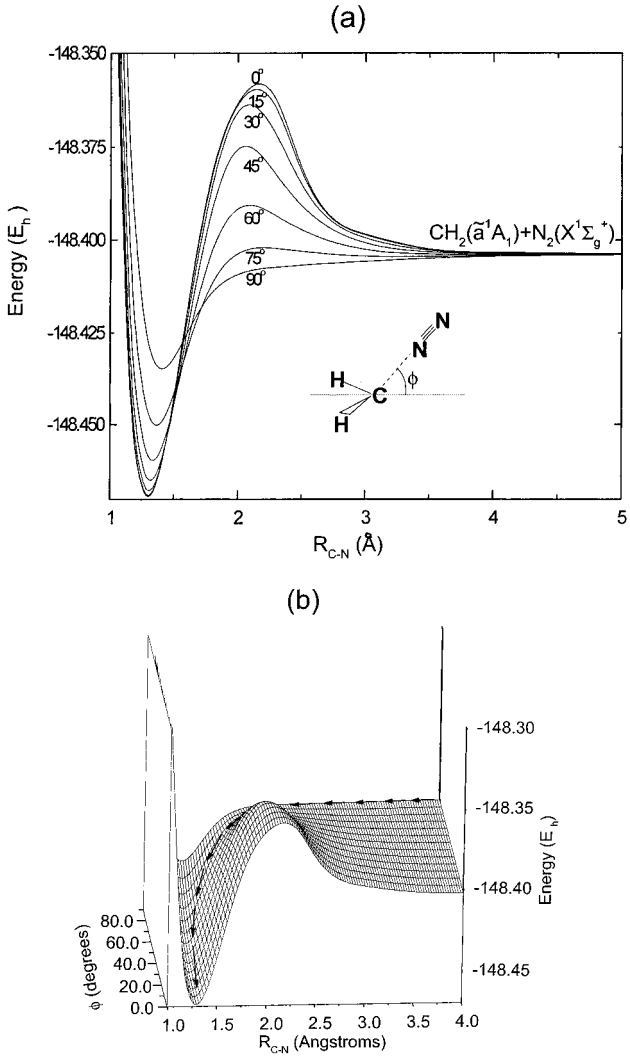

Figure 1. (a) Potential energy curves of the interaction CH_2 ($\tilde{a}^1A_1$) + N_2 ($X^1\Sigma_g^+$) for different ϕ angles. (b) Three-dimensional representation of (a).

where C_1, C_2, and C_1', C_2', are CAS variational coefficients with equilibrium values, C_1= 0.978, $C_2 = -0.208$, and $C_1' = 0.690$, $C_2' = 0.724$.

It is expected that the interaction of the ground $X^1\Sigma_g^+$ state of N_2 with the $\tilde{X}^3B_1$, and $\tilde{b}^1B_1$ states of CH_2 would be repulsive, (as has been, also, confirmed by low level calculations[10b,11]). The N_2 can interact attractively with the $\tilde{a}^1A_1$ and $\tilde{c}^1A_1$ states, either in a "π" fashion ($\tilde{a}^1A_1$, $|C_1|^2 = 0.98$) or in a "π" and "σ" fashion ($\tilde{c}^1A_1$, $|C_1'|^2 = 0.48$, $|C_2'|^2 = 0.52$). A σ-attack to the $\tilde{a}^1A_1$ state is expected to be repulsive or at least to present a significant energy barrier. Suppressing the small "C_2" component of the $\tilde{a}^1A_1$ state, the π-approach of the N_2 $X^1\Sigma_g^+$ state can be pictured by the following vbL icon:

$CH_2(\tilde{a}^1A_1) + N_2(X^1\Sigma_g^+) \rightarrow$ 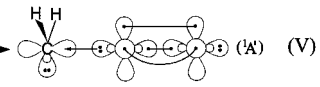 ($^1A'$) (V)

Figure 1a confirms the previous hypotheses. It shows the potential energy curves (PEC) of a series of attacks of $N_2(X^1\Sigma_g^+)$ to the $\tilde{a}^1A_1$ state of CH_2 parametrized with respect to the ϕ angle (see inset of Figure 1, $\phi = 0°$ defines the C_{2v} structure), at the

CASPT3 level. Along every PEC the ∠HCH angle was optimized, while keeping the other geometrical parameters of CH_2N_2 fixed at their CASPT2 equilibrium values. At $\phi = 90°$ (π-attack, icon V) no energy barrier is detected. As the $-N_2$ moiety approaches closer to the $\phi = 0°$ value (σ-attack), the energy barrier increases reaching a value of about 26 kcal/mol. Observe that the well depth of every PEC increases as the energy barrier increases with the global minimum corresponding to the $\phi = 0°$ value. It is interesting to report the variation of the ∠HCH angle along the PECs: asymptotically the ∠HCH angle is 102° ($\tilde{a}^1A_1$); moving toward the minimum of the $\phi = 90°$ PEC, the ∠HCH angle remains practically constant up to $r_{C-N} \cong 3$ Å, and then rises smoothly to a final value of about 113°. At the other extreme, along the $\phi = 0°$ PEC, the ∠HCH angle practically does not vary up to $r_{C-N} \cong 2.3$ Å. However, between $r_{C-N} = 2.3$ and 2.0 Å, the angle undergoes a dramatic change reaching a value of about 170° with a final value of 126° at the PEC minimum. The 170° value of the ∠HCH angle, at the top of the barrier, corresponds clearly to the $\tilde{c}^1A_1$ state of CH_2 (Table 1), indicating the heavy participation of this state to the binding mechanism of the CH_2N_2 system. Further support of the $\tilde{c}^1A_1$ involvement is provided by examining the CASSCF coefficients along the $\phi = 0°$ PEC at three characteristic r_{C-N} distances:

$r_{C\text{-}N} = \infty$,

$$\tilde{X}\,^1A_1(CH_2N_2) \sim \tilde{a}\,^1A_1(CH_2) \otimes X^1\Sigma_g^+(N_2) =$$

$$= \{0.98\,|\,\text{:C(H)(H)}\,\rangle - 0.21\,|\,\text{C(H)(H)}\,\rangle\} \otimes X^1\Sigma_g^+(N_2)$$

$r_{C\text{-}N} = 2.3$ Å,

corresponding leading configurations,

0.94 and -0.27,

$r_{C\text{-}N} = 2.0$ Å,

$$\tilde{X}\,^1A_1(CH_2N_2) \sim 0.98\,|\,\text{:N≡N:–C(H)(H)}\,\rangle$$

succinctly showing the entanglement of the "C_2'" component of the $\tilde{c}^1A_1$ CH_2 state around the $r_{C-N} = 2.0$ Å distance in the bonding CH_2-N_2 mechanism. Finally, at the global minimum ($r_{C-N} \cong 1.3$ Å), the leading configuration ($C \cong 0.98$) is the same as that at $r_{C-N} = 2.0$ Å, but the ∠HCH value decreases to 126°.

The above discussion is captured in Figure 1b, representing a three-dimensional representation of Figure 1a. The formation of CH_2N_2 from $CH_2(\tilde{a}^1A_1)$ and $N_2(X^1\Sigma_g^+)$ can be described as a "two step" *barrierless* process: a perpendicular π-attack ($\phi = 90°$) of N_2, followed by a relaxing of the system to a C_{2v} symmetry with an opening of the ∠HCH angle to ∼126°. The last step is possible due to the existence of the "C_2'" component (icon IV) of the $\tilde{c}^1A_1$ CH_2 state.

It is fair to say that the perpendicular π-attack of N_2 to the $\tilde{a}^1A_1$ CH_2 state was first mentioned by Lievin and Verhaegen.[10b]

Table 2 presents geometrical parameters and binding energies (D_e) of CH_2N_2 as obtained by CASPT2 and CASPT3 methods. With the exception of the CH_2N-N bond distance which differs by 0.011 Å from the experimental microwave value,[28] all other structural parameters are in very good agreement with the experiment. Observe that at the CASPT2 level of theory the ϕ angle of CH_2N_2 is 18.5° (C_s symmetry), while at the CASPT3 level is $\phi = 0°$ (C_{2v} symmetry). However, this bending mode is very "soft", the difference in energy between the C_{2v} and C_s ($\phi = 18.5°$) symmetries being less than 1 mhartree at the CASPT3 level.

TABLE 2: Total Energies *E* (hartrees), Geometrical Parameters (Bonds in angstroms, Angles in degrees), Dipole Moment μ (debye), and Dissociation Energies D_e (kcal/mol) of CH_2N_2

parameters	CASPT2	CASPT3	experiment[a]
E	−148.46228	−148.46935	
r_{N-N}	1.140	1.128	1.139
r_{N-C}	1.310	1.303	1.300
r_{C-H}	1.074	1.071	1.077
∠HCH	124.8	125.6	126.2
ϕ^b	18.5	0.0	0.0
∠NNC	182.2	180.0	180.0
μ	1.61		1.50 ± 0.01^c
D_e	42.0[d]	38.8[d]	<35[f], <44[g]
		38.2[d,e]	<41.7[h], 25[i]

[a] All geometrical parameters are from ref 28. [b] Out of plane CH_2-N_2 angle, see inset in Figure 1. [c] Reference 28. [d] With respect to $CH_2(\tilde{a}^1A_1) + N_2(X^1\Sigma_g^+)$. [e] Results obtained using the 12-to-12 reference space, see Methodology; the energy at this level but at the above CASPT3 geometry is −148.48232 hartree. [f] Pyrolysis, ref 22. [g] Electron impact, ref 23. [h] Photodissociation measurements, ref 25. [i] Reference 24.

Concerning the dissociation energy CH_2-N_2, it is obvious from Table 2 that the experimental situation is rather obscure. Not only the numerical values given differ significantly among each other, but it is unclear to what end products these values refer to, i.e., $\tilde{X}^3B_1$ or $\tilde{a}^1A_1$ of CH_2. Our CASPT2 and CASPT3 D_e values with respect to the asymptotic $CH_2(\tilde{a}^1A_1) + N_2(X^1\Sigma_g^+)$ fragments are 42.0 and 38.8 kcal/mol, respectively. The CASPT3 D_e value based on the 12e$^-$-to-12 orbital truncated CASSCF space (but using the CASPT3 geometries reported in Tables 1 and 2), is 38.2 kcal/mol differing by just 0.6 kcal/mol from the "small" CASPT3 calculation. Considering the 38.2 kcal/mol as our best value, a D_e=27.2 kcal/mol with respect to the $\tilde{X}^3B_1$ CH_2 state is obtained, by subtracting the 11.0 kcal/mol energy separation $\tilde{X}^3B_1 \leftarrow \tilde{a}^1A_1$ of CH_2, Table 1. This value is further decreased if the zero point energy (ZPE) difference is taken into account, $\Delta E(ZPE) = ZPE(N_2, X^1\Sigma_g^+) + ZPE(CH_2, \tilde{X}^3B_1) - ZPE(CH_2N_2) = 3.14 + 11.13 - 19.84 = -5.57$ kcal/mol, as obtained by a single reference MP2 calculation. Therefore, our D_0 value with respect to the $\tilde{X}^3B_1$ state of CH_2 is 21.6 kcal/mol. Possibly, a more accurate D_0 value could be obtained by considering the experimental value of the $\tilde{X}^3B_1-\tilde{a}^1A_1$ splitting of 9.22 kcal/mol (Table 1) instead of the 11.0 kcal/mol value used here, thus obtaining a $D_0 = 23.4$ kcal/mol.

For reasons of comparison we report that v. R. Schleyer et al.[16] give (with respect to the $\tilde{X}^3B_1$ CH_2 state) D_0=27.3 kcal/mol at the MP4SDTQ/6-31G*//MP2(full)/6-31G* level, while Kawauchi and co-workers[18] report a $D_0 = 19.4$ kcal/mol at the MP4SDTQ/6-31G**//MP2(full)/6-31G** level of theory.

Mulliken charges at the CASPT2 level are as follows:

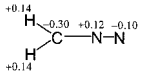

We see that the two moieties $-CH_2$ and $-N_2$ are essentially neutral; that is, no total charge transfer is observed from one fragment to the other. However, a close examination of the

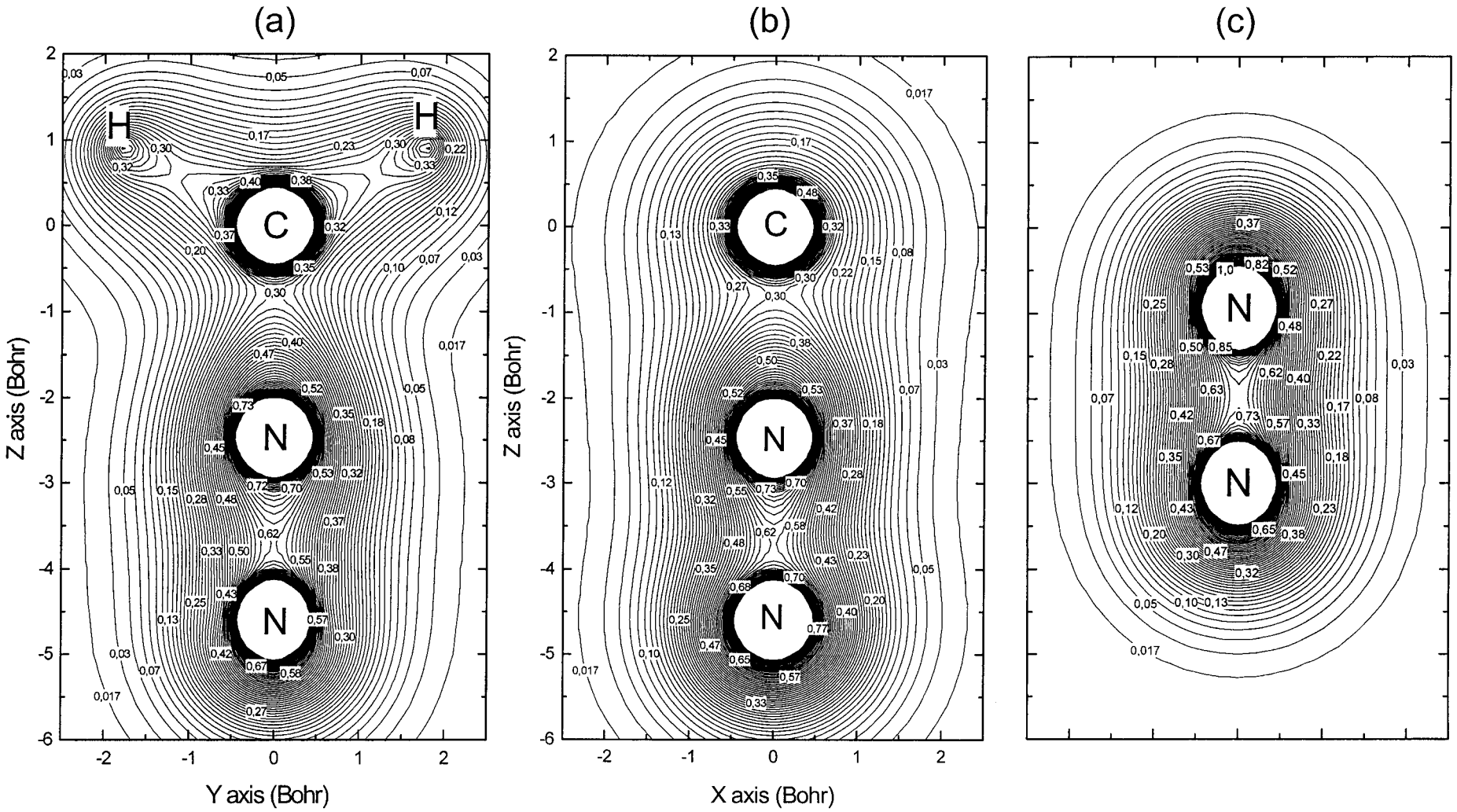

Figure 2. Total electron density contours (a) through the plane of CH_2N_2, (b) perpendicular to this plane, (c) of the free N_2 molecule.

atomic Mulliken distributions reveals that the central N-atom is losing $0.62e^-$ through its σ-frame due to the "harpooning" interaction represented by the following representation:

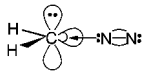

while at the same time the π-system of N_2 gains $0.62e^-$ with a concomitant lengthening of the N−N bond by 0.035 Å with respect to the free N_2 bond length. Figure 2 shows total electronic density contours (e^-/bohr^3): (a) through the plane (*yz*) of the molecule and (b) perpendicular to this plane and through the C, N, and N atoms. For reasons of comparison, analogous contours are also presented of the free N_2 molecule. Observe the σ-electron density displacement from N_2 toward the CH_2 fragment.

Final Remarks

With the purpose of elucidating the structural characteristics and binding mechanism of CH_2N_2, we have performed ab initio CASPT2 and CASPT3 calculations using correlation consistent TZ basis sets for all atoms. Our findings are summarized as follows: (1) The reaction $CH_2(\tilde{a}^1A_1) + N_2(X^1\Sigma_g^+) \rightarrow [CH_2N_2\ (^1A'; C_s)]^\ddagger \rightarrow CH_2N_2\ (\tilde{X}^1A_1; C_{2v})$ proceeds barrierlessly via a two step process due to the involvement of the $\tilde{c}^1A_1$ state of methylene. The absence of an energy barrier has been confirmed experimentally long ago.[38,39] (2) At the CASPT3 level we calculate a CH_2-N_2 D_e=38.2 kcal/mol with respect to the $\tilde{a}^1A_1$ CH_2 state and a D_0 = 23.4 kcal/mol with respect to the $\tilde{X}^3B_1$ CH_2 state. However, considering that the in situ $-CH_2$ moiety in CH_2N_2 finds itself in the *excited* $^1A_1$ state, the CH_2-N_2 "internal bond strength" corresponds to a D_e = 88.0 kcal/mol taking into account the energy separation between the $\tilde{a}$ and $\tilde{c}^1A_1$ states of CH_2, Table 1. (3) No need for in situ excited N_2 states and biradicals[9] or "hypervalent" states[20] are required; the binding mode in CH_2N_2 consists of a single σ-bond originating from the $\sigma(\sim 2s)$ electrons of central nitrogen and a π-like bond due to the back-transfer of the carbon π electrons. Similar thoughts have been expressed a quarter of century ago by Leroy and Sana[8] in the light of SCF calculations. The $-N_2$ triple bond in the molecule remains essentially intact as compared to the free N_2 system. Also, we would like to stress that, practically, no total charge transfer between the $-CH_2$ and $-N_2$ moieties is observed, that is these two entities inside the molecule are *neutral*. (4) Finally, and within our findings, a more consistent way of drawing the diazomethane molecule would be

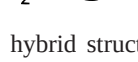

instead of the resonance hybrid structures which, indeed, do not correspond to any kind of "reality".

Acknowledgment. We thank Professor D. W. Setser for his remarks on the binding energy of CH_2N_2. This work was supported by the National and Kapodistrian University of Athens through Grant 70/4/3340.

References and Notes

(1) Fieser, L. F.; Fieser, M. *Advanced Organic Chemistry*; Reinhold Publishing Corporation: New York, 1961; p 376.
(2) Lide, D. R., Ed. *CRC Handbook of Chemistry and Physics*, 72nd ed.; CRC Press, Inc.: Boca Raton, 1991−1992. Interestingly enough, the well-known book by Vogel (ref 3), reports a boiling point of −24° C, while in the series of volumes, *Fieser's and Fieser's Reagents for Organic Synthesis*; John Wiley & Sons, Inc.: New York, 1967; Vol. I, p 191; a boiling point of −23 °C is mentioned.
(3) Vogel, A. I. *Vogel's Textbook of Practical Organic Chemistry*, 5th Ed.; Longmans: UK, 1989; p 430.
(4) Streitwieser, A., Jr.; Heathcock, C. H. *Introduction to Organic Chemistry*, 3rd ed.; Macmillan Publishing Company: New York, 1985; p 738.
(5) Huber, K. P.; Herzberg, G. *Molecular Spectra and Molecular Structure: IV. Constants of Diatomic Molecules*; Van Nostrand Reinhold: New York, 1979.
(6) Snyder, L. C.; Basch, H. *J. Am. Chem. Soc.* **1969**, *91*, 2189.
(7) Hart, B. T. *Aust. J. Chem* **1973**, *26*, 461 and 477.
(8) Leroy, G.; Sana, M. *Theor. Chim. Acta (Berlin)* **1974**, *33*, 329.
(9) Walsh, S. P.; Goddard, W. A., III *J. Am. Chem. Soc.* **1975**, *97*, 5319.
(10) (a) Lievin, J.; Verhaegen, G. *Theor. Chim. Acta* **1976**, 42, 47. (b) *Theor. Chim. Acta* **1977**, 45, 269.
(11) Bigot, B.; Ponec, R.; Sevin, A.; Devaquet, A. *J. Am. Chem. Soc.* **1978**, *100*, 6575.
(12) Sevin, A.; Bigot, B.; Devaquet, A. *Tetrahedron* **1978**, 34, 3275.
(13) Yamabe, S.; Minato, T.; Osamura, Y. *Int. J. Quantum Chem.* **1980**, 18, 243.
(14) Cooper, D. L.; Gerratt, J.; Raimondi, M.; Wright, S. C. *Chem. Phys. Lett.* **1987**, 138, 296.
(15) Cooper, D. L.; Gerratt, J.; Raimondi, M. *J. Chem. Soc., Perkin Trans. 2* **1989**, 1187.
(16) Boldyrev, A. I.; von R. Schleyer, P.; Higgins, D.; Thomson, C.; Kramarenko, S. S. *J. Comput. Chem.* **1992**, 13, 1066.
(17) Yamamoto, N.; Bernardi, F.; Bottoni, A.; Olivucci, M.; Robb, M. A.; Wilsey, S. *J. Am. Chem. Soc.* **1994**, *116*, 2064.
(18) Kawauchi, S.; Tachibana, A.; Mori, M.; Shibusa, W.; Yamabe, T. *J. Mol. Struct. (THEOCHEM)* **1994**, 310, 255.
(19) Habas, M.-p.; Dargelos, A. *Chem. Phys.* **1995**, 199, 177.
(20) Gerratt, J.; Cooper, D. L.; Karadakov, P. B.; Raimondi, M. *Chem. Soc. Rev.* **1997**, 87.
(21) Langer, A.; Hipple, J. A.; Stevenson, D. P. *J. Chem. Phys.* **1954**, 22, 1836.
(22) Setser, D. W.; Rabinovitch, B. S. *Can. J. Chem.* **1962**, *40*, 1425.
(23) Paulett, G. S.; Ettinger, P. E. *J. Chem. Phys.* **1963**, 39, 825 and 3534.
(24) Braun, W.; Bass, A. M.; Pilling, M. *J. Chem. Phys.* **1970**, 52, 5131.
(25) Laufer, A. H.; Okabe, H. *J. Am. Chem. Soc.* **1971**, *93*, 4137.
(26) Laufer, A. H.; Okabe, H. *J. Phys. Chem.* **1972**, *76*, 23.
(27) Chase, M. W., Jr.; Davies, C. A.; Downey, J. R., Jr.; Frurip, D. J.; McDonald, R. A.; Syverud, A. N. *J. Phys. Chem. Ref. Data Suppl.* **1985**, *1*.
(28) (a) Cox, A. P.; Thomas, L. F.; Sheridan, G. *Nature (London)* **1958**, 181, 1000. (b) Sheridan, G. *Adv. Mol. Spectrosc., Proc. IVth Int. Meet. Mol. Spectrosc.* **1962**, *1*, 139.
(29) Dunning, T. H., Jr. *J. Chem. Phys.* **1989**, *90*, 1007.
(30) Kendall, R. A.; Dunning, T. H., Jr.; Harrison, R. J. *J. Chem. Phys.* **1992**, *96*, 6796.
(31) Werner, H.-J. *Mol. Phys.* **1996**, *89*, 645.
(32) MOLPRO is a package of ab initio programs written by Werner, H.-J.; Knowles, P. J., with contributions from Almlof, J.; Amos, R. D.; Berning, A.; Deegan, M. J. O.; Eckert, F.; Elbert, S. T.; Hambel, C.; Lindh, R.; Meyer, W.; Nicklass, A.; Peterson, K.; Pitzer, R.; Stone, A. J.; Taylor, P. R.; Mura, M. E.; Pulay, P.; Schuetz, M.; Stoll, H.; Thorsteinsson, T.; Cooper, D. L.
(33) (a) Sherrill, C. D.; Van Huis, T. J.; Yamaguchi, Y.; Shaefer, H. F., III *J. Mol. Struct. (THEOCHEM)* **1997**, 400, 139. (b) Sherrill, C. D.; Leininger, M. L.; Van Huis, T. J.; Shaefer, H. F., III *J. Chem. Phys.* **1997**, *108*, 1040.
(34) Jensen, P.; Buenker, P. R. *J. Chem. Phys.* **1988**, *89*, 1327.
(35) Petek, H.; Nesbitt, D. J.; Darwin, D. C.; Ogilby, P. R.; Moore, C. B.; Ramsay, D. A. *J. Chem. Phys.* **1989**, *91*, 6566.
(36) Duxbury, G.; Jungen, C. *Mol. Phys.* **1988**, *63*, 981.
(37) Alijah, A.; Duxbury, G. *Mol. Phys.* **1990**, *70*, 605.
(38) Moore, C. B.; Pimentel, G. C. *J. Chem. Phys.* **1964**, *40*, 342.
(39) Milligan, D. E.; Jacox, M. E. *J. Chem. Phys.* **1967**, *47*, 5146.